



Published in final edited form as:

Cancer Res. 2015 January 1; 75(1): 147–158. doi:10.1158/0008-5472.CAN-14-0036.

Cables1 complex couples survival signaling to the cell death machinery

Zhi Shi^{#1,2}, Hae Ryon Park^{#2,5}, Yuhong Du^{2,4}, Zijian Li^{2,6}, Kejun Cheng^{2,7}, Shi-Yong Sun³, Zenggang Li², Haian Fu^{2,3,4}, and Fadlo R. Khuri^{3,4}

¹Department of Cell Biology & Institute of Biomedicine, College of Life Science and Technology, Jinan University, Guangzhou, China

²Department of Pharmacology, Emory University, Atlanta, Georgia 30322

³Department of Hematology & Medical Oncology and Winship Cancer Institute, Emory University, Atlanta, Georgia 30322

⁴Emory Chemical Biology Discovery Center, Emory University, Atlanta, Georgia 30322

⁵Department of Oral Pathology, School of Dentistry, Pusan National University, Pusan, South Korea

⁶Institute of Vascular Medicine, Peking University Third Hospital, Beijing, China

⁷Chemical Biology Center, Lishui Institute of Agricultural Sciences, Lishui, China

These authors contributed equally to this work.

Abstract

Cables1 is a candidate tumor suppressor that negatively regulates cell growth by inhibiting cyclin-dependent kinases. Cables1 expression is lost frequently in human cancer but little is known about its regulation. Here we report that Cables1 levels are controlled by a phosphorylation and 14-3-3 dependent mechanism. Mutagenic analyses identified two residues, T44 and T150, that are specifically critical for 14-3-3 binding and that serve as substrates for phosphorylation by the cell survival kinase Akt, which by binding directly to Cables1 recruits 14-3-3 to the complex. In cells Cables1 overexpression induced apoptosis and inhibited cell growth in part by stabilizing p21 and decreasing Cdk2 kinase activity. Ectopic expression of activated Akt prevented Cables1-induced apoptosis. Clinically, levels of phosphorylated Cables1 and phosphorylated Akt correlated with each other in human lung cancer specimens, consistent with pathophysiologic significance. Together, our results illuminated a dynamic regulatory system through which activated Akt and 14-3-3 work directly together to neutralize a potent tumor suppressor function of Cables1.

Corresponding authors: Haian Fu, Ph. D, Department of Pharmacology, Emory University, 1510 Clifton Road, Atlanta, GA 30322; hf@emory.edu, Phone: +1-404-275-0368, Fax: +1-404-275-0365; Fadlo R. Khuri, M. D, Department of Hematology & Medical Oncology, Emory University, 1365 Clifton Rd, NE, Ste 3000, Atlanta, GA 30322; fkhuri@emory.edu, Phone: +1-404-778-4250, Fax: +1-404-778-1267..

Disclosure statement

The authors declare no conflict of interest.

Keywords

Cables1; 14-3-3; Akt; apoptosis

Introduction

Cables1 (Cdk5 and Abl enzyme substrate 1) is a novel Cdk2, Cdk3, and Cdk5 binding protein, which acts as a link between the Cdks and nonreceptor tyrosine kinases and regulates the activity of Cdks by enhancing their Y15 phosphorylation (1, 2). In neurons, Cables1 promotes C-Abl to phosphorylate Cdk5 at Y15, resulting in increased kinase activity, and is believed to positively regulate neurite outgrowth. However, in proliferating cells, Cables connects Cdk2 and Wee1, which results in increased phosphorylation of Cdk2 at Y15, decreased kinase activity, and reduced cell proliferation. Cables1 interacts with p53 and p73 resulting in the induction of cell death (3), and also binds to TAp63 α to protect it from proteasomal degradation to ensure deletion of cells after genotoxic stress (4). Compared to Cables1^{+/+} MEFs, Cables1^{-/-} MEFs exhibit an increased growth rate, delayed senescence, and decreased serum dependence (5). Furthermore, Cables1^{-/-} mice have an increased incidence of endometrial cancer and a reduced survival rate in response to unopposed estrogen and colorectal cancer caused by 1,2-dimethylhydrazine (6, 7). Loss of Cables1 expression is observed with high frequency in human colon, lung, ovarian, and endometrial cancers (6, 8-10), and also enhances tumor progression in the *Apc*^{Min/+} mouse model and activates the Wnt/ β -catenin signaling pathway (11). Together, these observations suggest that Cables1 may function as a tumor suppressor. However, little is known about the regulation of Cables1 itself. It remains to be established how the growth suppressive function of Cables1 is coupled to cell survival and proliferative mechanisms. Our work revealed a signaling network interface by which Cables 1 is complexed with a phospho-Ser/Thr-recognition protein, 14-3-3, and its upstream kinase.

The 14-3-3 proteins are a highly conserved family of regulatory proteins expressed in all eukaryotic cells (12-16). In mammals, there are seven 14-3-3 isoforms (β , ν , ϵ , σ , ζ , γ , τ) encoded by distinct genes. 14-3-3 proteins function as dimers to bind to functionally diverse target proteins, including kinases, phosphatases, receptors, and molecular adaptors. 14-3-3 proteins regulate target proteins by cytoplasmic sequestration, occupation of interaction domains, prevention of degradation, activation/repression of enzymatic activity, and facilitation of protein modifications (12, 13, 15-18). Binding of 14-3-3s with target proteins is tightly regulated and the major mode of regulation is through reversible phosphorylation of target proteins within a defined motif. Two canonical 14-3-3 binding motifs have been identified as RSXpS/TXP (model I) and RXFXpS/TXP (model II), and a third C-terminal motif, pS/TX1-2-COOH (model III), has been defined (14, 19, 20). Within these motifs, phosphorylation of a specific serine (S) or threonine (T) residue is necessary for binding with 14-3-3. However, many target proteins do not contain sequences that accord precisely with these motifs, and some target proteins bind to 14-3-3 in a phosphorylation-independent manner. Interestingly, the consensus phosphorylation motif of the serine/threonine kinase Akt, RXRXXpS/T, partially overlaps with the sequences of mode I and II 14-3-3 binding motifs. Indeed, Akt phosphorylates many substrates within phosphorylation motifs, which

recruits 14-3-3 binding. Therefore, 14-3-3 binds to a number of Akt substrates and regulates various cell biological functions, including cell survival, proliferation, and metabolism. For example, Akt directly phosphorylates the Bcl-2 family member Bad on residue S136 and this creates a binding site for 14-3-3 proteins, which triggers release of Bad from its target proteins and inhibits the pro-apoptotic function of Bad (21-23). The FOXO transcription factors are also phosphorylated by Akt, which then recruits 14-3-3 binding and promotes their cytoplasmic retention. In this way, Akt prevents FOXO-induced target gene transcription that promotes apoptosis, cell-cycle arrest, and metabolic processes (24, 25). Thus, the identification and characterization of new protein targets that act downstream of Akt with coupled 14-3-3 binding may have significant biological and therapeutic implications.

Here, we present data to suggest a novel signaling mechanism by which Cables1 is suppressed by the combined actions of the Ser/Thr kinase, Akt, and the adaptor protein 14-3-3. Akt phosphorylation-mediated 14-3-3 binding prevents the apoptosis-inducing function of Cables1. Together, our data offer a new mechanism through which Cables1/Akt/14-3-3 interactions couple survival signaling to cell death.

Materials and Methods

Cells and reagents

COS7 and HEK293T cells were purchased from ATCC and maintained in DMEM with 10% fetal bovine serum and 100 units penicillin-streptomycin at 37°C in a humidified atmosphere of 5% CO₂. IGF-1, LY290024, Akt1/2 inhibitor and β-actin antibody were from Sigma-Aldrich. Anti-GST, HA, Akt, 14-3-3, pCDK(Y15), p57, cyclin A, cyclin D1, cyclin E, and Hsp90 antibodies were from Santa Cruz Biotechnology. Anti-pAkt substrate, pAkt S473, p21, p27, p53, pRb(S780), Rb, Bax, PARP, and GFP antibodies and recombinant Akt1 were from Cell Signaling Technologies. Anti-pCables1 T44 and T150 antibodies were generated by 21st Century Biochemicals.

Plasmids and transfection

Cables1 cDNAs were amplified by PCR and cloned into Gateway expression vectors (Invitrogen). Site-directed mutagenesis was performed using the QuikChange kit, following the manufacturer's protocol (Stratagene). Transfections were performed using FuGene HD (Roche).

Protein interaction assays

HexaHistidine (His)-affinity pull-down assay. Cells were lysed in His pull-down lysis buffer (1% Nonidet P-40, 137 mM NaCl, 1 mM MgCl₂, 40 mM Tris-Cl, 60 mM imidazole, 5 mM Na₄P₂O₇, 5 mM NaF, 2 mM Na₃VO₄, 1 mM phenylmethylsulfonyl fluoride, 10 mg/L aprotinin, 10 mg/L leupeptin). Lysates were cleared by centrifugation at 4°C. The clarified cell lysate was incubated with nickel-charged hexaHis resin for 2 hours at 4°C. The resin was washed two times with washing buffer (500 mM NaCl, 20 mM Tris-Cl, 60 mM imidazole) and once with binding buffer (500 mM NaCl, 20 mM Tris-Cl, 5 mM imidazole). Bound proteins were released from the resin by boiling in 6X SDS sample buffer for

Western blot analysis. *GST pull-down assay*. Cells were lysed in GST pull-down lysis buffer (1% Nonidet P-40, 150 mM NaCl, 100 mM Hepes, 5 mM Na₄P₂O₇, 5 mM NaF, 2 mM Na₃VO₄, 1 mM phenylmethylsulfonyl fluoride, 10 mg/L aprotinin, 10 mg/L leupeptin). Cleared cell lysates were incubated with glutathione-conjugated sepharose or the appropriate antibody and Protein G conjugated sepharose for 2 hours at 4°C. Then the resin was washed three times with GST pull-down lysis buffer and boiled in 6X SDS sample buffer for Western blot analysis. *Co-immunoprecipitation (Co-IP) assay*. Cells were lysed in Co-IP lysis buffer (1% Nonidet P-40, 150 mM NaCl, 100 mM Hepes, 5 mM Na₄P₂O₇, 5 mM NaF, 2 mM Na₃VO₄, 1 mM phenylmethylsulfonyl fluoride, 10 mg/L aprotinin, 10 mg/L leupeptin). Cleared cell lysates were incubated with Protein A or G conjugated sepharose (GE Healthcare) and the appropriate antibody for 2 hours to overnight at 4°C. Following incubation, the resin was washed three times with Co-IP lysis buffer and protein samples were eluted by boiling in 6× SDS sample buffer for Western blot analysis.

Akt1 and Cdk2 kinase assays

Recombinant active Akt1 (100 ng) was incubated with 10 µCi of [γ -³²P]ATP and 10 µg of recombinant Cables1 in 30 µl of kinase buffer (25 mM HEPES, 25 mM β-glycerophosphate, 25 mM MgCl₂, 2 mM dithiothreitol, 0.1 mM NaVO₃). To examine Cdk2 activity, Cdk2 isolated from lysates was incubated with 10 µCi of [γ -³²P]ATP and 5 µg of Histone H1 in 30 µl of kinase buffer (50 mM HEPES, 5 mM MgCl₂, 10 mM dithiothreitol). All reactions were incubated at 30 °C for 30 minutes and terminated by addition of 6X sample buffer. Proteins were separated by 10% SDS-PAGE, and phosphorylation was visualized by autoradiography.

Time resolved-Förster resonance energy transfer (TR-FRET) assays

Our published protocols for the TR-FRET assay were followed (26, 27). FITC-conjugated Cables1 T44 (FITC-Ahx-ENAPLRRCRTLSGSPR), T150 (FITC-Ahx-TNAFGARRNTIDSTSS), pT44 (FITC-Ahx-ENAPLRRCR (pT) LSGSPR) and pT150 (FITC-Ahx-TNAFGARRN (pT) IDSTSS) peptides were synthesized by Peptide 2.0 Inc (>80% purity). Bad pS136 was generated as described previously (28). Purified 6xHis tagged 14-3-3 proteins were indirectly labeled with terbium (Tb) fluorophore as a TR-FRET donor through a Tb conjugated anti-6xHis antibody (Cisbio Bioassays). The TR-FRET assay was performed in 384-well plates (30 µl/well). All assay components were diluted in assay buffer containing 20 mM Tris buffer, pH 7.5, 50 mM NaCl, and 0.01% Nonidet P-40. Briefly, increasing amounts of 14-3-3 proteins were mixed with Flu-labeled pT44, T44, pT150, T150 peptide, or pBad and incubated with anti-His-Tb antibody (50 ng/ml). After incubation at room temperature for 2 h, the TR-FRET signal was detected using an Envision Multilabel plate reader (PerkinElmer Life Sciences) with laser excitation at 337 nm, emissions at 486 nm and 520 nm, with a dual dichroic mirror (400/505 nm). The delay time was set at 50 µs. The TR-FRET signal is expressed as the TR-FRET signal ratio: F520nm/F486nm * 10⁴, where F520 nm and F486 nm are fluorescence counts at 520 nm and 486 nm for fluorescein and Tb, respectively. The TR-FRET signal window was calculated as the difference between the TR-FRET signal values for bound Flu-peptide in the presence of 14-3-3 protein and values for unbound Flu-peptide in the absence of 14-3-3 protein. All experimental data were analyzed using Prism 5.0 software (Graphpad Software).

14-3-3 γ affinity chromatography for identification of 14-3-3 binding partners

14-3-3 binding protein identification from A549 lung cancer cells, including the discovery of Cables1 as a novel 14-3-3 partner, is described in the Supplementary Materials section.

Western blot

Proteins were separated on 12.5% SDS-PAGE gels and transferred to PVDF membranes. Membranes were blocked with 5% BSA and incubated with the indicated primary antibodies. Corresponding horseradish peroxidase-conjugated secondary antibodies (Santa Cruz Biotechnology) were used against each primary antibody. Proteins were detected using West-Pico or West-Dura enhanced chemiluminescent detection reagents (Pierce) and a Kodak imaging system or films.

Apoptosis assay

Cells were stained with Annexin V-PE (BD), then analyzed with a Guava flow cytometer (Millipore) to determine the percentage of apoptotic cells.

Immunofluorescence assay

Cells were fixed with 2% paraformaldehyde for 30 minutes, and permeabilized with 0.1% Triton X-100 for 20 minutes, then blocked with 1% bovine serum albumin for 1 hour. Rabbit anti-C-PARP antibody (Cell Signaling Technologies) was added and incubated for 1 hour. After washing with PBS, cells were incubated with goat anti-rabbit IgG conjugated with Texas Red (Invitrogen) and 1 μ g/ml Hoechst 33342 (Promega). Cells were then imaged with an ImageXpress 5000 (Molecular Devices).

Immunohistochemistry assay

Formalin-fixed, paraffin-embedded human lung cancer tissue array slides (ABXIS and Biochain) were stained with anti-pCables1 T44, T150 (21st Century), and pAkt S473 (Epitomics) antibodies using a microwave-enhanced avidin-biotin staining method. For quantitation of protein expression, the following formula was used: IHC score = % positive cells \times intensity score. The intensity was scored as follows: 0, negative; 1, weak; 2, moderate; and 3, intense. An IHC score of 100 or greater was considered positive.

Statistical analysis

A student's t-test was used to compare individual data points among each group. Correlation was analyzed using Fisher's exact test. A *P* value of less than 0.05 was set as the criterion for statistical significance.

Results

Cables1 interacts with 14-3-3

To discover critical signaling nodes at the junction of cell survival and death, we utilized 14-3-3 protein as a molecular probe in an affinity capture-based proteomics study to explore novel 14-3-3 binding proteins and their regulation (Supplementary Materials; (29)). Our proteomics analysis in A549 lung cancer cells identified known 14-3-3 binding partners

detected the levels of GST-Cables1 in His pull-down complexes. As shown in Figure 1F, GST-Cables1 binding to His-14-3-3 γ was dose-dependently enhanced with gradually increasing calyculin A concentrations. These data support the importance of regulated phosphorylation dictating the interaction of Cables1 with 14-3-3.

Cables1 binds 14-3-3 through T44 and T150 sites

The binding of 14-3-3 to target proteins is generally mediated through RSXpS/TXP and RXXXpS/TXP motifs where pS/T represents phosphoserine or phosphothreonine (17). To explore which binding motifs in Cables1 mediate its binding with 14-3-3, we first generated two truncations of Cables1, 1-200 and 201-368, and tested their interaction with 14-3-3. GST-Cables1 truncation 1-200 or 201-368 and His-14-3-3 γ were co-transfected into COS7 cells and His pull-down and Western blot analysis were performed. As shown in Figure 2A, truncation 1-200 was able to bind to His-14-3-3 γ , while truncation 201-368 did not bind to His-14-3-3 γ . This result indicates the binding sites on Cables1 that are required for interaction with 14-3-3 are located within residues 1-200 of Cables1. Next, we searched for conserved sequences in Cables1 using ScanSite (www.scansite.com) and identified several potential 14-3-3 binding sites including T44, S46, S48, and S169. To determine which of the predicted S/T residues are true 14-3-3 binding sites, we mutated all S/T residues to alanine (A) and examined the binding of these mutants with 14-3-3 in His-14-3-3 γ pull-down assays. As shown in Figure 2B, compared with WT, a decreased interaction with 14-3-3 was shown for the two Cables1 single mutants, T44A and T150A. The other alanine mutants of Cables1 did not affect its interaction with 14-3-3. To test whether both T44 and T150 sites are involved in the binding of Cables1 to 14-3-3, we made two double mutants T44A/T150A (AA) and T44D/T150D (DD) of Cables1 and examined their binding to 14-3-3 using the same binding assay. The DD mutant was made to test if it may mimic the phosphorylation status of Cables1. The binding of GST-Cables1 AA and DD with His-14-3-3 γ were clearly weaker than that of Cables1 WT (Figure 2C). These data suggest that the T44 and T150 sites likely mediate the binding of Cables1 with 14-3-3. As the DD mutant did not interact with 14-3-3, we assume that the DD mutant did not mimic the phosphorylated state of Cables1 required for 14-3-3 binding.

If the T44- and T150-containing regions of Cables1 directly bind 14-3-3, these isolated peptides may be able to compete for the interaction of full length Cables with 14-3-3. To test this, we performed a competitive binding assay by pre-incubating the peptides derived from Cables1 with lysates overexpressing GST-Cables1 and His-14-3-3 γ followed by His-14-3-3 γ pull-down assay. Figure 2D shows that both phosphorylated T44 and T150 peptides effectively disrupted the interaction of Cables1 with 14-3-3, while non-phosphorylated T44 and T150 peptides showed significantly reduced effect on the Cables1/14-3-3 interaction at the highest concentration (50 μ M). The positive control Bad pS136 peptide and R18, which specifically bind to the amphipathic groove of 14-3-3 with high affinity, completely blocked the binding of GST-Cables1 with His-14-3-3 γ at 10 μ M. Next, we tested whether these Cables1 peptides can directly interact with 14-3-3 protein in a defined *in vitro* system using a homogenous TR-FRET assay (26). The TR-FRET assay provides a sensitive measurement for proximity based molecular interactions to evaluate the binding of the donor-fluorophore (Tb)-coupled 14-3-3 proteins with FITC-labeled Cables1 peptides. Because the stringent

requirement of $<100 \text{ \AA}$ distance between donor and acceptor fluorophores, the generation of a dose-dependent FRET signal usually suggests a direct interaction of between two test proteins. Indeed, the incubation of phosphorylated Cables1 pT44 peptide (FITC-pT44) with Tb-14-3-3 γ induced a dose-dependent increase of TR-FRET signal, suggesting a direct interaction of 14-3-3 γ with the pT44 peptide (Figure 2E). As in the competition assay, unphosphorylated T44 was unable to bind and generated low TR-FRET signal, suggesting the importance of phosphorylation in enhancing the affinity of the T44 peptide to 14-3-3. This effect was not limited to the γ isoform, as similar TR-FRET signals of FITC-pT44 were induced with 14-3-3 ν (Figure 2E, right panel). Then, the interaction of the pT150 peptide was also tested. The pT150 peptide interacted with both the γ and ν isoforms of 14-3-3 tested as evident by robust dose-dependent TR-FRET signals. Conversely, unphosphorylated T150 peptide had generated negligible TR-FRET signal (Figure 2F). These data strongly suggest that phosphorylated T44 and T150 peptides can directly bind to 14-3-3 proteins, and that phosphorylation at these residues is required for Cables1 binding to 14-3-3.

Taken together, these results indicate that Cables1 may require both pT44 and pT150 sites for effective binding with 14-3-3, possibly through a coordinated fashion (16). Moreover, both T44 and T150 sites are highly conserved among a variety of species, further supporting the potential importance of these two sites through evolution (data not shown).

Akt phosphorylates Cables1 at 14-3-3 binding sites

The two 14-3-3 binding sites on Cables1, T44 and T150, reside in sequences that overlap with consensus motifs for potential Akt phosphorylation. To test the hypothesis that Akt phosphorylates Cables1 and then recruits 14-3-3 binding, we examined the effect of WT and kinase dead (KD) Akt1 on the binding of Cables1 to 14-3-3. HA-Akt1 WT or KD was co-transfected with GST-Cables1 and His-14-3-3 γ into COS7 cells, then His pull-down assay and Western blot were carried out. Akt1 WT significantly enhanced the binding of GST-Cables1 and His-14-3-3 γ , while Akt1 KD moderately decreased their binding (Figure 3A). Next, we used a general anti-pAkt substrate antibody that recognizes the motif RXXXpS/T to detect phosphorylated levels of Cables1 WT and various single mutants in GST-Cables1 pulled-down complexes. As shown in Figure 3B, both Cables1 T44A and T150A single mutants showed significantly lower levels of pAkt substrate recognition, while other Cables1 single mutants showed levels equal to Cables1 WT. To specifically detect the phosphorylated level of Cables1 T44 and T150, we generated corresponding anti-pCables1 T44 and T150 antibodies. The levels of pCables1 T44 and pCables1 T150 were equal for all Cables1 variants except the T44A and T150A mutants, respectively, which showed significantly reduced levels (Figure 3B). We also used the same methods to examine the phosphorylated levels of the Cables1 AA and DD mutants when co-expressed with Akt1 WT or KD. Phosphorylated levels of GST-Cables1 WT were clearly increased when Akt1 WT was overexpressed and were decreased when Akt1 KD was overexpressed, but phosphorylated levels of the Cables1 AA and DD mutants were significantly reduced and even undetectable under certain conditions (Figure 3C). Next, we assessed the interaction between Akt1 and Cables1 by detecting HA-Akt1 WT and KD levels in GST, GST-Cables1 WT or GST-Cables1 AA complexes which were pulled-down from their overexpressing lysates. HA-Akt1 WT and KD were detectable in GST-Cables1 WT or GST-Cables1 AA

complexes but not in GST complexes, and HA-Akt1 WT and KD showed equal interactions with GST-Cables1 WT and the AA mutant (Figure 3D). To test whether endogenous Akt can also phosphorylate Cables1, we activated endogenous Akt by treating serum-starved GST-Cables1 overexpressing cells with IGF-1 and detecting phosphorylated levels of pulled-down GST-Cables1. As shown in Figure 3E, activating endogenous Akt with IGF-1 markedly enhanced the phosphorylated levels of GST-Cables1. This enhancement was totally blocked by pretreating cells with the PI3K inhibitor, LY294002, or AKT1/2 inhibitor. To further examine whether Akt is able to phosphorylate Cables1 directly, we performed an *in vitro* radio-labeling kinase assay using recombinant Akt1 and GST-Cables1 WT, T44A, T150A, and AA mutants. The autoradiography results demonstrated that Cables1 WT was effectively phosphorylated by Akt, showing significant labeling with ³²P. While mutations in Cables1, T44A and T150A, decreased the labeling of ³²P signals of GST-Cables1, the GST-Cables1 AA double mutant exhibited the greatest reduction in Cables1 phosphorylation (Figure 3F). Additionally, Western blot analysis detected pCables1 T44 only with GST-Cables1 WT and T150 mutants, and pCables1 T150 only with GST-Cables1 WT and T44 mutants (Figure 3F). Together, these data suggest that Akt is an upstream kinase that phosphorylates Cables1 at T44 and T150 sites.

Cables1 overexpression induces apoptosis

Cables1 has been reported to enhance p53-induced cell death in U2OS cells (3). Overexpressing Cables1 alone could also induce apoptosis in several ovarian cancer cells (32). To determine the role of the 14-3-3 binding sites in Cables1 induced apoptosis, we overexpressed control Venus, Venus-Cables1 WT, and AA in HEK293T cell. Apoptosis of Venus-positive cells was analyzed by detecting Annexin V-positive cells as well as cleaved PARP levels by Western blot. As shown in Figures 4A and 4B, overexpressing Venus-Cables1 WT induced apoptosis and PARP cleavage in a dose- and time-dependent manner, while overexpressing Venus-Cables1 AA induced more apoptosis and PARP cleavage than WT under the same conditions. We also examined the level of intracellular cleaved PARP by immunofluorescence assay. Compared with Venus overexpressing cells, Venus-Cables1 WT and AA overexpressing cells showed a significantly increased level of intracellular cleaved PARP (Figure 4C). These data suggest that Akt phosphorylation and 14-3-3 binding might control Cables1-induced apoptosis. To investigate the possible molecular mechanism by which Cables1 AA induces more apoptosis than WT, we tested their effects on Cdk2 Y15 phosphorylation level and kinase activity. Cdk2 was immunoprecipitated from the lysates of Venus, Venus-Cables1 WT, and AA overexpressing HEK293T cells. Cdk2 kinase activity was detected by *in vitro* radiolabeling kinase assay with histone H1 as the substrate, and the interaction of Cdk2 with Venus-Cables1 was analyzed by Western blot. As shown in Figure 4D, compared with WT, Cables1 AA showed greater interaction with Cdk2, increased Cdk2 Y15 phosphorylation, and decreased Cdk2 kinase activity. Furthermore, we examined the levels of several cell cycle regulatory proteins in the lysates of Venus, Venus-Cables1 WT, and AA overexpressing HEK293T cells, and found that Cables1 AA induced higher p21 and lower phosphorylated Rb protein levels than Cables1 WT. No changes were observed in the protein levels of Bax, p53, p27, p57, cyclin A, cyclin D1, or cyclin E (Figure 4E).

Activated Akt prevents apoptosis induced by Cables1

The above data suggest that the Akt phosphorylation sites of Cables1 may modulate its inhibition of Cdk2, the stability of p21, and the apoptosis induction activity of Cables1. Next, we determined the effects of Akt on apoptosis induced by Cables1. We co-expressed Venus, Venus-Cables1 WT, and AA as well as HA-Akt1 WT and KD in HEK293T cells and analyzed induction of apoptosis as above. As shown in Figure 5A, overexpressing HA-Akt1 WT significantly inhibited apoptosis and PARP cleavage induced by Venus-Cables1 WT, but moderately inhibited apoptosis and PARP cleavage induced by Venus-Cables1 AA. In contrast, overexpressing HA-Akt1 KD increased apoptosis and PARP cleavage in Venus, Venus-Cables1 WT, and AA overexpressing cells. We also inactivated endogenous Akt by withdrawing serum from the culture medium of Venus, Venus-Cables1 WT and AA overexpressing HEK293T cells and analyzed cell apoptosis. As shown in Figure 5B, endogenous pAkt S473 levels, which indicate endogenous Akt activity, decreased with increasing serum-starvation time. Apoptosis and PARP cleavage in Venus, Venus-Cables1 WT, and AA overexpressing HEK293T cells were enhanced with increasing serum-starvation time. These results suggest that activated Akt is able to prevent apoptosis induced by Cables1.

The level of pCables1 is correlated with that of pAkt in human lung cancer patient and A549 xenograft mouse model tissues

The above results demonstrate that Cables1 is phosphorylated by Akt in cell culture. To determine whether this is also the case in tumor tissues, we compared the levels of pCables1 T44, T150, and pAkt S473 in 37 human lung cancer samples by immunostaining with the corresponding antibodies. Information about sex, age, histology, and IHC results of the samples are summarized in Supplementary Table S2, and the IHC images of three representative samples are shown in Figure 6A. While sample 1 showed negative staining of pCables1 T44, T150 and pAkt S473, Sample 2 showed positive pAkt S473 staining with negative staining of pCables1 T44 and T150, and Sample 3 showed positive staining of pCables1 T44, T150, and pAkt S473. The results from the IHC analysis are summarized in Figure 6B. Positive pAkt S473 staining was present in 13 out of 37 patient tumor tissue samples. Interestingly, positive pCables1 T44 and T150 staining was only present in 9 out of 37 samples. Importantly, all 9 samples also showed positive pAkt S473 staining, suggesting that the levels of pCables1 T44 and T150 in human lung cancer tissues might be controlled by the same mechanism as the activated Akt level. Together, these results in human lung cancer specimens confirm our observations in cell-culture experiments, and indicate that the level of pCables1 is correlated with that of pAkt, supporting a potentially significant role in lung cancer tumorigenesis.

These studies led to our working model (Figure 7) and suggest that Cables1 growth inhibition activity is antagonized by oncogenic kinases, such as Akt, through phosphorylation of Cables1 at T44 and T150. To test this model, we examined whether Akt status was correlated with Cables1 phosphorylation at these two sites *in vivo* using a lung cancer A549 xenograft mouse model (33). As shown in Figure S1, tumors treated with vehicle showed relatively high Akt phosphorylation at T473 along with phosphorylated Cables1 at T44 and T150. Conversely, tumors treated with a mTOR kinase inhibitor,

INK128, exhibited reduced Akt pT473, and showed decreased phosphorylation of Cables1 at T44 and T150. When tumors were treated with INK128 and a GSK3beta inhibitor, SB216763, both the Akt phosphorylation level and the Cables1 phosphorylation level were reversed. Band intensity information was captured by normalizing pAkt and Cables1 at pT44 and pT150 against pan-Akt and Cables1. The statistical analysis (MatLab, corcoef) of these data led to $p = 0.009$ for pAKT/pT44 of Cables1 with a correlation coefficient (R) of 0.717 and $p = 0.001$ for pAKT/pT150 of Cables1 (R = 0.832), suggesting highly significant correlation between phosphorylation level of Akt and Cables1 at these sites further supporting the proposed working model in Figure 7.

Discussion

In the present study, we identified a critical mechanism that regulates Cables1 function by which the cell growth inhibition activity, and thus the tumor suppression activity, of Cables1 is suppressed by activated Akt and Akt phosphorylation-induced 14-3-3 binding. We have identified Cables1 as a new 14-3-3 interacting protein and demonstrated that their interaction is phosphorylation-dependent and mediated by the T44 and T150 sites of Cables1. While motif-scanning shows that T44 (not T150) is a classical 14-3-3 binding motif, our mutational results suggest that both of these sites mediate 14-3-3 binding, although the binding of synthesized peptides with 14-3-3 *in vitro* indicates that the Cables1 pT44 peptide binds 14-3-3 more potently than the Cables1 pT150 peptide. Structural analysis of 14-3-3 dimers has revealed that each monomer contains an independent target-protein binding region; therefore the dimer can interact with two motifs simultaneously, belonging to either a single protein or separate binding partners. Such binding through two sites allows intricate signal transmission and network coordination (16). The binding of the T44 and T150 sites of Cables1 with 14-3-3 most likely occurs in such a coordinated fashion.

We have identified Akt as one kinase that can directly bind to and phosphorylate Cables1, and recruit 14-3-3 binding. Akt, also known as protein kinase B (PKB), is a central node in cell signaling downstream of growth factors, cytokines, and other cellular stimuli. Activated Akt phosphorylates many protein substrates and thus has diverse roles in several cellular processes, including cell survival, growth, proliferation, angiogenesis, metabolism, and migration (35). In addition to Cables1, Akt phosphorylates several Cables1-related proteins and induces their interaction with 14-3-3. Akt is able to phosphorylate Wee1 and promote its cytoplasmic localization by binding to 14-3-3. Re-localized Wee1 cannot phosphorylate Cdk1 and Cdk2 at Y15 sites, which relieves their kinase activity and promotes cell cycle progress (36). Akt also phosphorylates Cdk2 and causes its cytoplasmic localization through interaction with 14-3-3. This Cdk2 cytoplasmic redistribution is required for cell progression from S to G2-M phase (37). Several groups have reported that Akt also phosphorylates the Cdk inhibitor p27, resulting in its cytosolic sequestration via 14-3-3 binding. Inhibiting p27 nuclear localization enhances its degradation and attenuates its cell cycle inhibitory effects (38-40). Similarly, Akt phosphorylates another Cdk inhibitor, p21, which, like p27, leads to p21 cytosolic localization by interaction with 14-3-3 (41). Recently, one component of the SCF^{Skp2} ubiquitin ligase complex Skp2, which mediates ubiquitination and degradation of several cell cycle related proteins including p21 and p27, was shown to be phosphorylated by Akt. Skp2 phosphorylation by Akt enhances its stability through disrupting the

interaction between Cdh1 and Skp2, then triggers SCF^{Skp2} complex formation and E3 ligase activity, also leading to 14-3-3-dependent Skp2 relocalization to the cytosol (42, 43). In contrast to these Akt substrates, we did not observe any changes in the localization and stability of Cables1 by Akt-mediated phosphorylation and 14-3-3 binding. Our results showed that Akt phosphorylation and 14-3-3 binding prevented the function of Cables1 in the induction of apoptosis. Although Cables1 has been reported to enhance p53-induced cell death in U2OS cells and to induce apoptosis in several ovarian cancer cells (3, 32), the exact molecular mechanism by which Cables1 induces apoptosis is still unclear. In this study, we found that Cables1 inhibits the kinase activity of Cdk2 by increasing the pCdk2 Y15 level, which is consistent with a previous report (1). Interestingly, our study also showed that Cables1 increases the level of p21 and decreases the level of pRb, but does not affect the other cell cycle-related proteins we studied. Cdk2 and p21 play critical roles in the control of apoptosis by regulating the function of several apoptosis-related proteins, such as Foxo1, ASK1, and c-Myc (44, 45). Therefore, the inhibition of Cdk2 and upregulation of p21 by Cables1 may contribute to its induction of apoptosis. Moreover, Cables1 AA had stronger effect than WT on decreasing Cdk2 activity and pRb level, increasing p21 level and inducing apoptosis, indicating that these functions of Cables1 are controlled by the phosphorylation status of T44 and T150 residues, which are phosphorylated by Akt. Indeed, expressing exogenous Akt prevents Cables1-induced apoptosis, while inactivated endogenous Akt potentiates Cables1-induced apoptosis. Thus, in tumor cells with activated Akt, it is possible that the tumor suppressor function of Cables1 is neutralized through phosphorylation of T44 and T150. In support of this, we observed a correlation between the expression of pCables1 and pAkt in cultured cells, in human lung cancer patient samples, and in tumor tissues of an A549 xenograft mouse model. Our working model proposes that under growth conditions, survival signals activate Akt which in turn phosphorylates Cables1 and recruits 14-3-3 binding (Figure 7) to prevent the induction of apoptosis by Cables1, which occurs partially through inhibiting Cdk2 activity and upregulating p21.

In summary, we have discovered a critical regulatory mechanism of the tumor suppressor Cables1, which we have newly identified as an Akt substrate and 14-3-3 binding protein. Akt phosphorylation-mediated 14-3-3 binding prevents the apoptosis-inducing function of Cables1. Our findings also suggest a central role of Cables1 in coupling upstream survival signals to the cell death machinery. It is possible that activated Akt in cancer may neutralize the tumor suppressor function of Cables1, which in turn leads to uncontrolled cell growth and tumorigenesis. Thus, the Akt/14-3-3/Cables1 protein-protein interaction interfaces may be targeted to release Cables1 to assume its growth inhibition activity for potential therapeutic discovery.

Supplementary Material

Refer to Web version on PubMed Central for supplementary material.

Acknowledgement

We would like to thank past and present members of the Fu/Khuri laboratory for many stimulating discussions. We thank Drs LR Zukerberg and BR Rueda (Massachusetts General Hospital) for sharing reagents, Dr Andrei Ivanov for statistical analysis, and Drs Anthea Hammond and Cheryl Meyerkord-Belton for editing the text. This work was

supported by National Institutes of Health grants P01 CA116676 (to H.F. and F.R.K.), Georgia Cancer Coalition (to H.F. and F.R.K.), Winship Cancer Institute Kennedy Seed grant (Y.D), and following grants to Z.S.: the Chinese National Natural Science Foundation No. 31271444 and No. 81201726, the Foundation for Research Cultivation and Innovation of Jinan University No. 21612407, the Science and Technology Program of Guangzhou No. 14200010, and the Specialized Research Fund for the Doctoral Program of Higher Education No. 20124401120007.

References

1. Wu CL, Kirley SD, Xiao H, Chuang Y, Chung DC, Zukerberg LR. Cables enhances cdk2 tyrosine 15 phosphorylation by Wee1, inhibits cell growth, and is lost in many human colon and squamous cancers. *Cancer research*. 2001; 61:7325–32. [PubMed: 11585773]
2. Zukerberg LR, Patrick GN, Nikolic M, Humbert S, Wu CL, Lanier LM, et al. Cables links Cdk5 and c-Abl and facilitates Cdk5 tyrosine phosphorylation, kinase upregulation, and neurite outgrowth. *Neuron*. 2000; 26:633–46. [PubMed: 10896159]
3. Tsuji K, Mizumoto K, Yamochi T, Nishimoto I, Matsuoka M. Differential effect of ik3-1/cables on p53- and p73-induced cell death. *J Biol Chem*. 2002; 277:2951–7. [PubMed: 11706030]
4. Wang N, Guo L, Rueda BR, Tilly JL. Cables1 protects p63 from proteasomal degradation to ensure deletion of cells after genotoxic stress. *EMBO Rep*. 2010; 11:633–9. [PubMed: 20559324]
5. Kirley SD, Rueda BR, Chung DC, Zukerberg LR. Increased growth rate, delayed senescence and decreased serum dependence characterize cables-deficient cells. *Cancer Biol Ther*. 2005; 4:654–8. [PubMed: 15908791]
6. Zukerberg LR, DeBernardo RL, Kirley SD, D'Apuzzo M, Lynch MP, Littell RD, et al. Loss of cables, a cyclin-dependent kinase regulatory protein, is associated with the development of endometrial hyperplasia and endometrial cancer. *Cancer research*. 2004; 64:202–8. [PubMed: 14729625]
7. Kirley SD, D'Apuzzo M, Lauwers GY, Graeme-Cook F, Chung DC, Zukerberg LR. The Cables gene on chromosome 18Q regulates colon cancer progression in vivo. *Cancer Biol Ther*. 2005; 4:861–3. [PubMed: 16210915]
8. Dong Q, Kirley S, Rueda B, Zhao C, Zukerberg L, Oliva E. Loss of cables, a novel gene on chromosome 18q, in ovarian cancer. *Mod Pathol*. 2003; 16:863–8. [PubMed: 13679449]
9. Park do Y, Sakamoto H, Kirley SD, Ogino S, Kawasaki T, Kwon E, et al. The Cables gene on chromosome 18q is silenced by promoter hypermethylation and allelic loss in human colorectal cancer. *Am J Pathol*. 2007; 171:1509–19. [PubMed: 17982127]
10. Tan D, Kirley S, Li Q, Ramnath N, Slocum HK, Brooks JS, et al. Loss of cables protein expression in human non-small cell lung cancer: a tissue microarray study. *Hum Pathol*. 2003; 34:143–9. [PubMed: 12612882]
11. Arnason T, Pino MS, Yilmaz O, Kirley SD, Rueda BR, Chung DC, et al. Cables1 is a tumor suppressor gene that regulates intestinal tumor progression in Apc(Min) mice. *Cancer Biol Ther*. 2013; 14:672–8. [PubMed: 23792637]
12. Aitken A. 14-3-3 proteins: a historic overview. *Semin Cancer Biol*. 2006; 16:162–72. [PubMed: 16678438]
13. Freeman AK, Morrison DK. 14-3-3 Proteins: diverse functions in cell proliferation and cancer progression. *Seminars in cell & developmental biology*. 2011; 22:681–7. [PubMed: 21884813]
14. Muslin AJ, Tanner JW, Allen PM, Shaw AS. Interaction of 14-3-3 with signaling proteins is mediated by the recognition of phosphoserine. *Cell*. 1996; 84:889–97. [PubMed: 8601312]
15. Tinti M, Johnson C, Toth R, Ferrier DE, Mackintosh C. Evolution of signal multiplexing by 14-3-3-binding 2R-ohnologue protein families in the vertebrates. *Open biology*. 2012; 2:120103. [PubMed: 22870394]
16. Yaffe MB. How do 14-3-3 proteins work?--Gatekeeper phosphorylation and the molecular anvil hypothesis. *FEBS Lett*. 2002; 513:53–7. [PubMed: 11911880]
17. Fu H, Subramanian RR, Masters SC. 14-3-3 proteins: structure, function, and regulation. *Annu Rev Pharmacol Toxicol*. 2000; 40:617–47. [PubMed: 10836149]
18. Porter GW, Khuri FR, Fu H. Dynamic 14-3-3/client protein interactions integrate survival and apoptotic pathways. *Semin Cancer Biol*. 2006; 16:193–202. [PubMed: 16697216]

19. Yaffe MB, Rittinger K, Volinia S, Caron PR, Aitken A, Leffers H, et al. The structural basis for 14-3-3:phosphopeptide binding specificity. *Cell*. 1997; 91:961–71. [PubMed: 9428519]
20. Coblitz B, Shikano S, Wu M, Gabelli SB, Cockrell LM, Spieker M, et al. C-terminal recognition by 14-3-3 proteins for surface expression of membrane receptors. *J Biol Chem*. 2005; 280:36263–72. [PubMed: 16123035]
21. Masters SC, Yang H, Datta SR, Greenberg ME, Fu H. 14-3-3 inhibits Bad-induced cell death through interaction with serine-136. *Mol Pharmacol*. 2001; 60:1325–31. [PubMed: 11723239]
22. Zha J, Harada H, Yang E, Jockel J, Korsmeyer SJ. Serine phosphorylation of death agonist BAD in response to survival factor results in binding to 14-3-3 not BCL-X(L). *Cell*. 1996; 87:619–28. [PubMed: 8929531]
23. Datta SR, Dudek H, Tao X, Masters S, Fu H, Gotoh Y, et al. Akt phosphorylation of BAD couples survival signals to the cell-intrinsic death machinery. *Cell*. 1997; 91:231–41. [PubMed: 9346240]
24. Brunet A, Bonni A, Zigmond MJ, Lin MZ, Juo P, Hu LS, et al. Akt promotes cell survival by phosphorylating and inhibiting a Forkhead transcription factor. *Cell*. 1999; 96:857–68. [PubMed: 10102273]
25. Brunet A, Kanai F, Stehn J, Xu J, Sarbassova D, Frangioni JV, et al. 14-3-3 transits to the nucleus and participates in dynamic nucleocytoplasmic transport. *J Cell Biol*. 2002; 156:817–28. [PubMed: 11864996]
26. Du Y, Fu RW, Lou B, Zhao J, Qui M, Khuri FR, et al. A time-resolved fluorescence resonance energy transfer assay for high-throughput screening of 14-3-3 protein-protein interaction inhibitors. *Assay and drug development technologies*. 2013; 11:367–81. [PubMed: 23906346]
27. Gunther JR, Du Y, Rhoden E, Lewis I, Revenaugh B, Moore TW, et al. A set of time-resolved fluorescence resonance energy transfer assays for the discovery of inhibitors of estrogen receptor-coactivator binding. *Journal of biomolecular screening*. 2009; 14:181–93. [PubMed: 19196699]
28. Du Y, Masters SC, Khuri FR, Fu H. Monitoring 14-3-3 protein interactions with a homogeneous fluorescence polarization assay. *Journal of biomolecular screening*. 2006; 11:269–76. [PubMed: 16699128]
29. Pozuelo Rubio M, Geraghty KM, Wong BH, Wood NT, Campbell DG, Morrice N, et al. 14-3-3 affinity purification of over 200 human phosphoproteins reveals new links to regulation of cellular metabolism, proliferation and trafficking. *The Biochemical journal*. 2004; 379:395–408. [PubMed: 14744259]
30. Fujii K, Goldman EH, Park HR, Zhang L, Chen J, Fu H. Negative control of apoptosis signal-regulating kinase 1 through phosphorylation of Ser-1034. *Oncogene*. 2004; 23:5099–104. [PubMed: 15094778]
31. Goldman EH, Chen L, Fu H. Activation of apoptosis signal-regulating kinase 1 by reactive oxygen species through dephosphorylation at serine 967 and 14-3-3 dissociation. *J Biol Chem*. 2004; 279:10442–9. [PubMed: 14688258]
32. Sakamoto H, Friel AM, Wood AW, Guo L, Ilic A, Seiden MV, et al. Mechanisms of Cables 1 gene inactivation in human ovarian cancer development. *Cancer Biol Ther*. 2008; 7:180–88. [PubMed: 18059193]
33. Koo J, Yue P, Gal AA, Khuri FR, Sun SY. Maintaining glycogen synthase kinase-3 activity is critical for mTOR kinase inhibitors to inhibit cancer cell growth. *Cancer research*. 2014; 74:2555–68. [PubMed: 24626091]
34. Ren H, Chen M, Yue P, Tao H, Owonikoko TK, Ramalingam SS, et al. The combination of RAD001 and NVP-BKM120 synergistically inhibits the growth of lung cancer in vitro and in vivo. *Cancer Lett*. 2012; 325:139–46. [PubMed: 22781393]
35. Manning BD, Cantley LC. AKT/PKB signaling: navigating downstream. *Cell*. 2007; 129:1261–74. [PubMed: 17604717]
36. Katayama K, Fujita N, Tsuruo T. Akt/protein kinase B-dependent phosphorylation and inactivation of WEE1Hu promote cell cycle progression at G2/M transition. *Mol Cell Biol*. 2005; 25:5725–37. [PubMed: 15964826]
37. Maddika S, Ande SR, Wiehac E, Hansen LL, Wesselborg S, Los M. Akt-mediated phosphorylation of CDK2 regulates its dual role in cell cycle progression and apoptosis. *J Cell Sci*. 2008; 121:979–88. [PubMed: 18354084]

38. Liang J, Zubovitz J, Petrocelli T, Kotchetkov R, Connor MK, Han K, et al. PKB/Akt phosphorylates p27, impairs nuclear import of p27 and opposes p27-mediated G1 arrest. *Nat Med.* 2002; 8:1153–60. [PubMed: 12244302]
39. Shin I, Yakes FM, Rojo F, Shin NY, Bakin AV, Baselga J, et al. PKB/Akt mediates cell-cycle progression by phosphorylation of p27(Kip1) at threonine 157 and modulation of its cellular localization. *Nat Med.* 2002; 8:1145–52. [PubMed: 12244301]
40. Viglietto G, Motti ML, Bruni P, Melillo RM, D'Alessio A, Califano D, et al. Cytoplasmic relocation and inhibition of the cyclin-dependent kinase inhibitor p27(Kip1) by PKB/Akt-mediated phosphorylation in breast cancer. *Nat Med.* 2002; 8:1136–44. [PubMed: 12244303]
41. Zhou BP, Liao Y, Xia W, Spohn B, Lee MH, Hung MC. Cytoplasmic localization of p21Cip1/WAF1 by Akt-induced phosphorylation in HER-2/neu-overexpressing cells. *Nat Cell Biol.* 2001; 3:245–52. [PubMed: 11231573]
42. Lin HK, Wang G, Chen Z, Teruya-Feldstein J, Liu Y, Chan CH, et al. Phosphorylation-dependent regulation of cytosolic localization and oncogenic function of Skp2 by Akt/PKB. *Nat Cell Biol.* 2009; 11:420–32. [PubMed: 19270694]
43. Gao D, Inuzuka H, Tseng A, Chin RY, Toker A, Wei W. Phosphorylation by Akt1 promotes cytoplasmic localization of Skp2 and impairs APCCdh1-mediated Skp2 destruction. *Nat Cell Biol.* 2009; 11:397–408. [PubMed: 19270695]
44. Huang H, Regan KM, Lou Z, Chen J, Tindall DJ. CDK2-dependent phosphorylation of FOXO1 as an apoptotic response to DNA damage. *Science.* 2006; 314:294–7. [PubMed: 17038621]
45. Abbas T, Dutta A. p21 in cancer: intricate networks and multiple activities. *Nat Rev Cancer.* 2009; 9:400–14. [PubMed: 19440234]

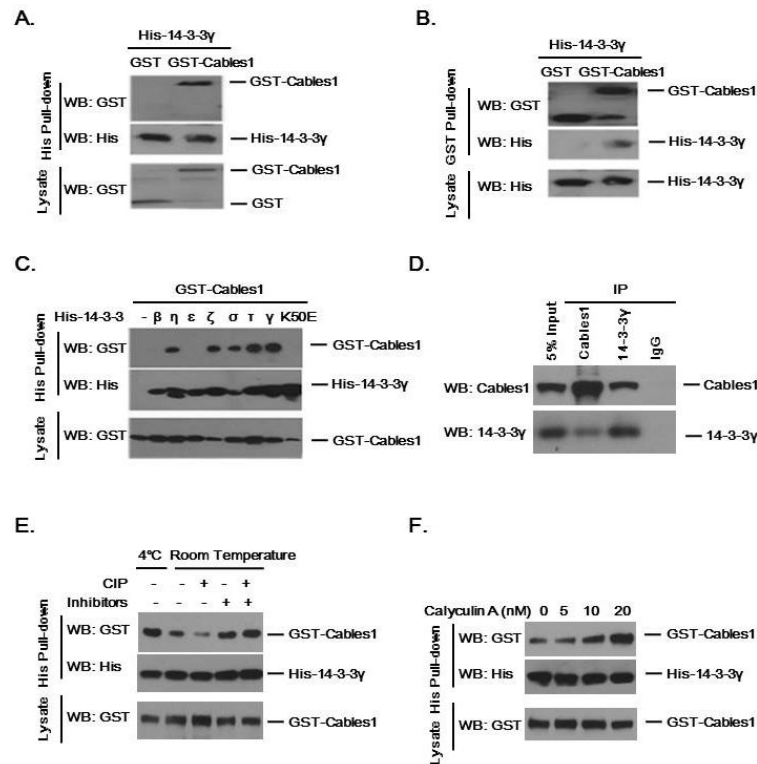


Figure 1. Cables1 interacts with 14-3-3

(A) Cables1 interacts with 14-3-3 γ in a His-14-3-3 pull-down assay (B) 14-3-3 γ binds to Cables1 in a GST-Cables1 pull-down assay. COS7 cells were transfected with His-14-3-3 γ , GST, or GST-Cables1. After 2 days, cells were lysed and His pull-down and GST pull-down were performed. Proteins were examined by Western blot. (C) Cables1 preferentially binds to 14-3-3 isoforms ν , σ , ζ , γ , and τ . The presence of GST-Cables1 was examined in each His-14-3-3 isoform complex from co-transfected cell lysates. (D) Endogenous Cables1 and 14-3-3 γ interact with each other. Endogenous Cables1 and 14-3-3 γ were immunoprecipitated from PC12 cells in two directions and detected reciprocally. (E) Phosphatase inhibitors enhance the binding of 14-3-3 with Cables1. Cell lysates with co-expressed His-14-3-3 γ and GST-Cables1 were incubated with or without CIP or phosphatase inhibitors (5 mM Na₄P₂O₇, 5 mM NaF, 5 mM Na₃VO₄) for 0.5 h at room temperature, then GST-Cables1 was detected in His-14-3-3 γ complexes. (F) Calyculin A enhances the binding of 14-3-3 with Cables1. Cells overexpressing His-14-3-3 γ and GST-Cables1 were treated with the indicated amount of calyculin A for 1 h, then GST-Cables1 was examined in His-14-3-3 γ complexes.

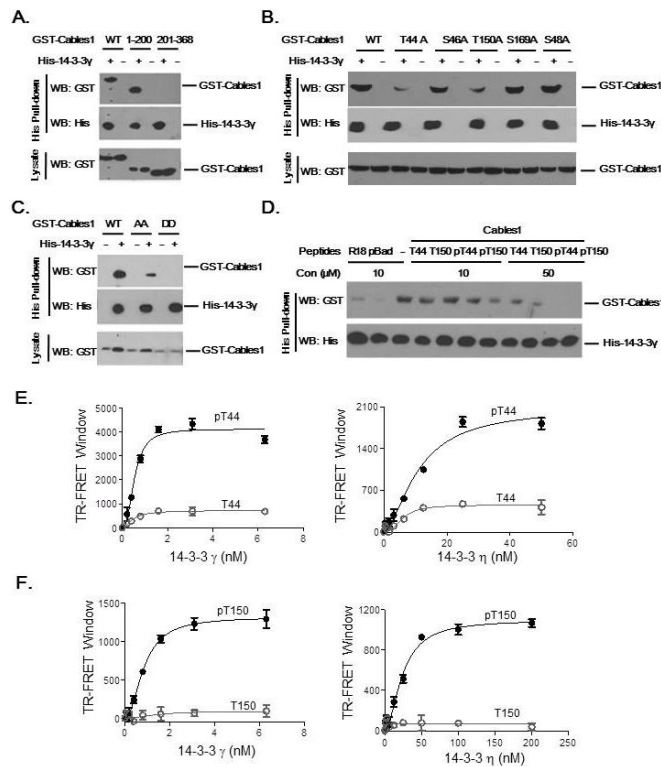


Figure 2. Cables1 interacts with 14-3-3 through T44 and T150 sites

(A) Cables1 truncation mutant 1-200 interacts with 14-3-3. (B) Mutations in T44 and T150 of Cables1, not other tested sites, decrease 14-3-3 binding. (C) Double mutants T44/T150AA and DD of Cables1 exhibit decreased binding to 14-3-3. COS7 cells were co-transfected with His-14-3-3 γ and the indicated GST-Cables1 variants. His-14-3-3 γ complexes were pulled-down from cell lysates and GST-Cables1 variants were detected by Western blot. (D) Cables1 pT44 and pT150 peptides block the binding of Cables1 with 14-3-3. The indicated peptides were incubated with lysates overexpressing GST-Cables1 and His-14-3-3 γ for 1 h. GST-Cables1 was detected in His-14-3-3 isoform complexes. (E) Direct binding of the pT44 peptide of Cables1 to 14-3-3 γ (left) and 14-3-3 η (right). (F) Direct binding of the pT150 peptide of Cables1 to 14-3-3 γ (left) and 14-3-3 η (right). TR-FRET titration assays were carried out in triplicate in a 384-well plate with 5 nM Cables1 peptides and increasing 14-3-3 concentrations for 2 h. The TR-FRET assay window was calculated as described in the *Materials and Methods*. Both unphosphorylated T44 and T150 peptides were included for comparison.

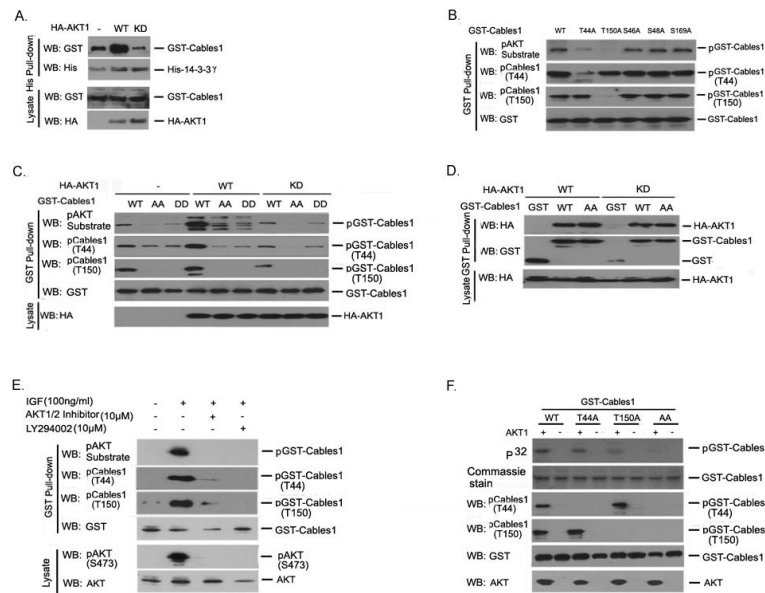


Figure 3. Akt phosphorylation of Cables1 recruits 14-3-3 binding

(A) Akt enhances the binding of Cables1 with 14-3-3. His-14-3-3 γ complexes were pulled-down from cell lysates overexpressing His-14-3-3 γ , GST-Cables1, and HA-Akt1 WT or KD, followed by SDS-PAGE and Western blot with the indicated antibodies. (B) Mutations in T44 and T150 of Cables1 abolish its phosphorylation by Akt. Each GST-Cables1 variant was isolated from transfected cells and detected by the indicated antibodies. (C) Exogenous Akt phosphorylates Cables1. Phosphorylation of GST-Cables1 WT, AA, and DD was examined in cells overexpressing HA-Akt1 WT or KD. (D) Akt interacts with Cables1. COS7 cells were co-transfected with HA-Akt1 WT or KD and GST or GST-Cables1 WT. After 48h, cells were lysed, GST pull-down was performed, and proteins were detected by Western blot. (E) Endogenous AKT phosphorylates Cables1. Cells were transfected with GST-Cables1, and after 24 h, cells were serum-starved for 24 h. Cells were treated with or without 10 μ M Akt1/2 inhibitor or 10 μ M LY290024 for 1 h followed by 100 ng/ml IGF for 15 mins. Cells were lysed and phosphorylation of GST-Cables1 was measured in the isolated GST-Cables1 complex. (F) Akt phosphorylates Cables1 *in vitro*. The indicated recombinant proteins were incubated with or without recombinant Akt1 in kinase buffer containing [γ - 32 P]ATP at 30°C for 0.5 h. Proteins were separated by SDS-PAGE, followed by autoradiography, Coomassie stain, or Western blot.

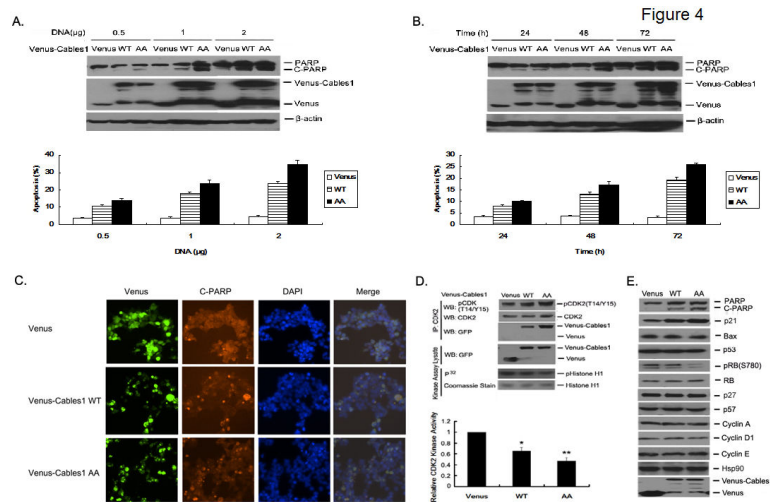


Figure 4. Cables1 overexpression induces cell apoptosis

(A) Cables1 overexpression dose-dependently induces apoptosis. HEK293T cells in 12-well plates were transfected with increasing amounts of Venus, Venus-Cables1 WT, or AA. After 72 hours, cells were lysed and proteins were detected by Western blot. Cells were stained with Annexin V-PE and induction of apoptosis in Venus-positive cells was analyzed by flow cytometry. (B) Cables1 overexpression time-dependently induces apoptosis. HEK293T cells in 12-well plates were transfected with 1 μ g Venus, Venus-Cables1 WT, or AA. After the indicated times, protein detection and apoptosis analysis were performed as in (A). (C) Cables1 overexpression induces increased intracellular cleaved PARP. Venus, Venus-Cables1 WT, and AA overexpressing cells were stained with rabbit anti-C-PARP antibody and goat anti-rabbit IgG with conjugated Texas Red and Hoechst 33342. Images were taken with an ImageXpress 5000. (D) Cables1 overexpression inhibits Cdk2 activity. Cdk2 was immunoprecipitated from the lysates of Venus, Venus-Cables1 WT, or AA overexpressing cells, then used in a kinase assay. Proteins were detected by Western blot. * and ** represent $P < 0.05$ and $P < 0.01$ respectively, for values versus those in the control Venus group. (E) Cables1 overexpression increases p21 and decreases pRb levels. Lysates of Venus, Venus-Cables1 WT, and AA overexpressing cells were used to examine the indicated proteins levels by Western blot.

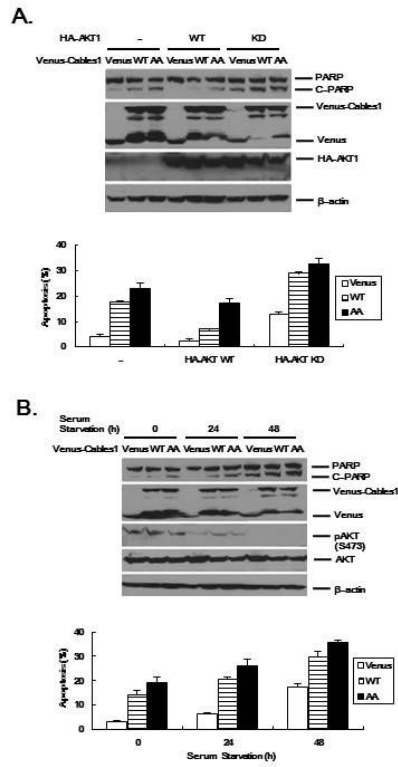


Figure 5. Activated Akt prevents apoptosis induced by Cables1

(A) Akt overexpression prevents apoptosis induced by Cables1. HEK293T cells were co-transfected with Venus, Venus-Cables1 WT, and AA as well as HA-Akt1 WT and KD. After 72 hours, cells were lysed and proteins were detected by Western blot. Cells were also stained with Annexin V-PE and apoptosis of Venus positive cells was analyzed by flow cytometry. (B) Inactivating endogenous Akt enhances apoptosis induced by Cables1. HEK293T cells were transfected with Venus, Venus-Cables1 WT, and AA, then serum was withdrawn for the indicated times. Protein detection and apoptosis analysis conducted as in (A).

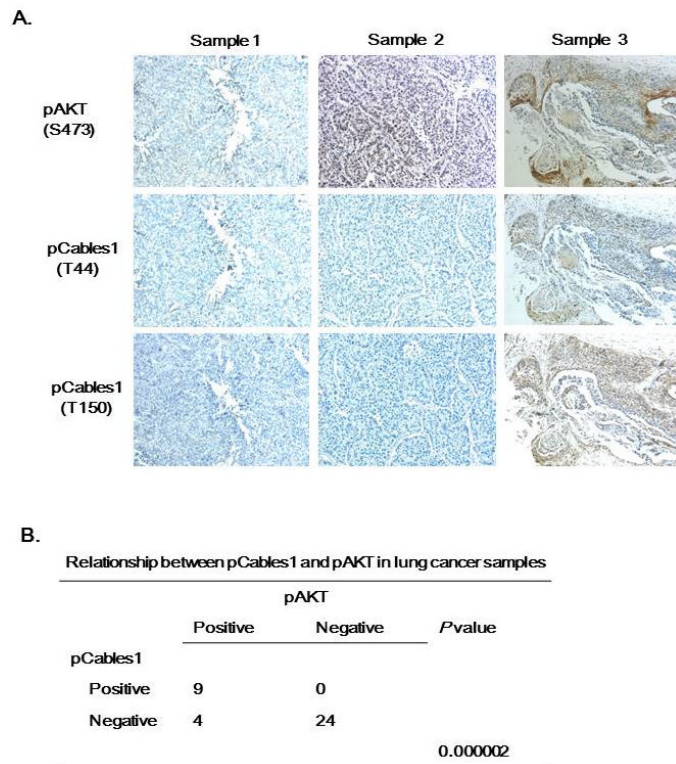


Figure 6. The level of pCables1 correlates with that of pAkt in human lung cancer patient tissues (A) Immunohistochemical staining of human lung cancer patient tissues was performed with the indicated antibodies. Staining of three representative samples is shown. (B) A summary of the results is shown. Correlation between the levels of pCables1 and pAkt was analyzed using Fisher's exact test.

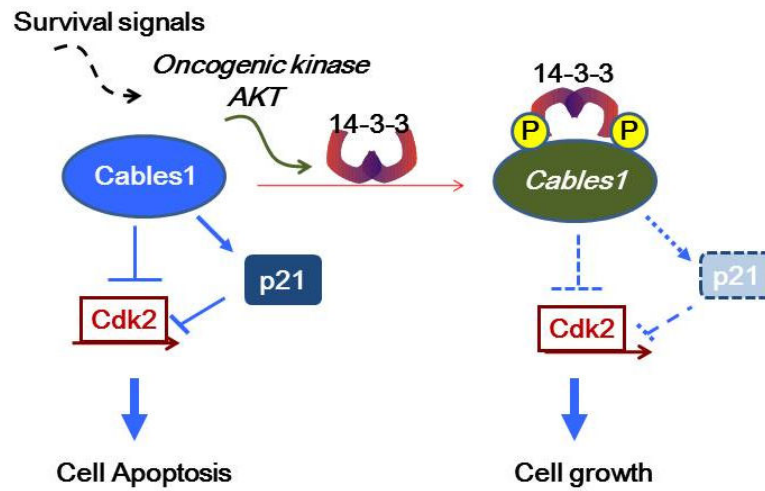


Figure 7. Akt phosphorylation and 14-3-3 binding regulate Cables1-mediated induction of apoptosis

Under growth conditions, survival signals activate Akt, which in turn phosphorylates Cables1 and recruits 14-3-3 binding. Induction of apoptosis by Cables1, which occurs partially through inhibiting Cdk2 activity and upregulating p21, is prevented by Akt phosphorylation and 14-3-3 binding.